Journal of Hazardous Materials 170 (2009) 744–753

Contents lists available at ScienceDirect

Journal of Hazardous Materials

journal homepage: www.elsevier.com/locate/jhazmat

Effect of the adsorbate (Bromacil) equilibrium concentration in water on its adsorption on powdered activated carbon. Part 1. Equilibrium parameters

Fadi Al Mardini [1], Bernard Legube *

Université de Poitiers, CNRS, Laboratoire de Chimie et Microbiologie de l'Eau (UMR 6008), Ecole Supérieure d'Ingénieurs de Poitiers, 40 avenue du Recteur Pineau, 86022 Poitiers Cedex, France

ARTICLE INFO

Article history:
Received 9 February 2009
Received in revised form 25 March 2009
Accepted 6 May 2009
Available online 14 May 2009

Keywords:
Adsorption
Equilibrium
Water
PAC
Bromacil

ABSTRACT

This study was carried out to investigate the adsorption equilibrium and kinetics of a pesticide of the uracil group on powdered activated carbon (PAC). The experiments were conducted at a wide range of initial pesticide concentrations (~5 μg L^{-1} to ~500 μg L^{-1} at pH 7.8), corresponding to equilibrium concentrations of less than 0.1 μg L^{-1} for the weakest, which is compatible with the tolerance limits of drinking water. Such a very broad range of initial solute concentrations resulting powdered activated carbon (PAC) concentrations (0.1–5 mg L^{-1}) is the main particularity of our study. The application of several monosolute equilibrium models (two, three or more parameters) has generally shown that Bromacil adsorption is probably effective on two types of sites. High reactivity sites ($K_L \sim 10^3$ L mg^{-1}) which are 10–20 less present in a carbon surface than lower reactivity sites ($K_L \sim 10$ L mg^{-1}), according to the q_m values calculated by two- or three-parameter models. The maximum capacity of the studied powdered activated carbon (PAC), corresponding to monolayer adsorption, compared to the Bromacil molecule surface, would be between 170 mg g^{-1} and 190 mg g^{-1}. This theoretical value is very close to the experimental q_m values obtained when using linearized forms of Langmuir, Tóth and Fritz–Schluender models.

1. Introduction

When treating surface water to obtain drinking water, filtration on granular activated carbon (GAC) is a process that is used worldwide, especially at the end of treatment, after clarification of water (coagulation, flocculation, decantation, sand filtration) and ozonation, before final disinfection by chlorine (or derivatives). Over the last two decades, GAC filtration has been frequently replaced, at the same waterworks level, by adsorption on powdered activated carbon (PAC) coupled with liquid–solid separation (lamellar decantation, microfiltration or ultrafiltration). The PAC doses used, in this case, are a few mg/L. Crystal® and Carboflux® are the best known processes in France running on this principle. Regardless of how the activated carbon is implemented, the main objective of this drinking water treatment phase is to eliminate organic micropollutants (such as pesticides) in order to achieve very low residual concentrations. European regulations specify a maximum concentration of 0.1 μg L^{-1} for each pesticide (and related products) in water intended for human consumption [1]. Most academic studies on the adsorption of chemical compounds in aqueous solution on PAC are generally carried out with initial chemical compound concentrations of a few mg/L or more. In these studies, the range of initial chemical compound concentrations is often fairly reduced. Moreover, these compounds are generally simple aromatic compounds (i.e. phenols) or even dyes. These potential pollutants and their concentration are usually selected on the basis of analytical considerations. However, it is hard or even impossible to apply the published results in industrial conditions, particularly with respect to pesticides at concentrations of a few μg L^{-1}. Moreover, concerning activated carbon, the chosen experimental variable is generally the adsorbent mass, seldom the initial solute concentration. As for pesticides, many academic and applied research studies have obviously been published on the adsorption of atrazine at very low concentrations especially in natural water [2,3] or in the presence of natural organic matter [4–6].

This study was carried out to assess the adsorption equilibrium and kinetics of a pesticide of the uracil group on powdered activated carbon at a wide range of initial pesticide concentrations corresponding to minimum equilibrium concentration values of less than 0.1 μg L^{-1}, which is compatible with drinking water tolerance limits.

This publication presents the results of the most academic part of some experiments on PAC adsorption of a pesticide in buffered pure water, and their interpretation according to known models. The determined equilibrium constants (part 1) and kinetic con-

* Corresponding author. Tel.: +33 5 49453917; fax: +33 5 49453768.
E-mail addresses: almardinifadi@yahoo.fr (F. Al Mardini), Bernard.legube@univ-poitiers.fr (B. Legube).
[1] University of Damascus, Faculty of Sciences, Department of Chemistry, Al Baramkeh, Damascus, Syria.

0304-3894/$ – see front matter © 2009 Elsevier B.V. All rights reserved.
doi:10.1016/j.jhazmat.2009.05.003

Nomenclature

$B_T = q_m RT/\Delta Q$	constant in Temkin isotherm
C_e	Bromacil concentration at equilibrium ($mg\,L^{-1}$, $\mu g\,L^{-1}$)
C_s	solute solubility ($mg\,L^{-1}$)
C_0	initial Bromacil concentration ($mg\,L^{-1}$, $\mu g\,L^{-1}$)
$K_d = q_e/C_e$	distribution coefficient ($L\,g^{-1}$)
K_E	Elovich equilibrium constant ($L\,mg^{-1}$)
K_F	Freundlich constant indicative of the relative adsorption capacity of the adsorbent ($mg^{(1-n)}\,L^n\,g^{-1}$)
K_L	Langmuir equilibrium constant ($L\,mg^{-1}$)
K_T	Temkin equilibrium constant ($L\,mg^{-1}$)
m	PAC mass (g)
$m_s = m/V$	PAC concentration ($g\,L^{-1}$)
n	Freundlich constant indicative of the intensity of the adsorption
PAC	powdered activated carbon
q_0	solute concentration initially present on PAC ($mg\,g^{-1}$)
q_e	PAC surface complex concentration at equilibrium ($mg\,g^{-1}$)
q_m	maximum adsorption capacity from Langmuir ($mg\,g^{-1}$)
q_{mDR}	maximum adsorption capacity in the micropores from Dubinin-Radushkevich ($mg\,g^{-1}$)
T	absolute temperature (K)
TOC	total organic carbon
V	solution volume (L)
ΔQ	variation of adsorption energy ($J\,mol^{-1}$)

Greek letters

β	constant of adsorption energy $E = 1/(\beta)^{0.5}$
ε	potentiel of Polanyi = $RT\ln(C_s/C_e)$
θ	surface coverage (q_e/q_m)

stants (part 2) should ultimately be useful for studies on adsorption in real water (containing natural organic material as co-adsorbate), and for defining the essential needs to better design industrial installations.

The pesticide studied was Bromacil. This herbicide is used to control perennial grasses, brush, and weeds on non-agricultural land. It is also used for selective weeding in citrus and pineapple crop fields [7]. Bromacil is not photodegradable on the soil surface, stable to photolysis in water, except under alkaline conditions, stable to hydrolysis in water between pH 5 and 9 [8] and soluble in water, so it may be readily leached into the soil and thus contaminate groundwater [9]. It has been found in groundwater in Florida, at 300 $\mu g\,L^{-1}$ [10], and more recently in natural waters of Martinique at concentrations of up to 2 $\mu g\,L^{-1}$ in the presence of other pesticides, such as chlordecon, hexachlorocyclohexane beta (HCH-β) and aldicarb derivatives [11].

2. Materials and methods

2.1. Equilibrium experiments

A similar protocol was used for all equilibrium isotherm experiments, but with three different reactors according to the studied concentration ranges:

- experiments in two perfectly agitated and thermostated reactors with a maximum volume of 5 L or 15 L, respectively for the high and medium Bromacil concentrations,
- experiments in an agitated and nonthermostated 250 L reactor, for very low Bromacil concentrations.

2.1.1. Isotherm for high and medium Bromacil concentrations

The Bromacil mother solution was prepared in ultrapure water (18 $M\Omega\,cm^{-1}$, TOC $\leq$ 0.1 $mg\,C\,L^{-1}$) at a concentration below the solubility limit reported in the literature. No organic solvent was used to increase the Bromacil solubility. The daughter solutions were prepared by dilution with the same water, buffered with sodium phosphate salts (NaH_2PO_4, H_2O and Na_2HPO_4), to achieve a final ionic strength of 1.75×10^{-3} M. The final pH of the studied solution was adjusted to 7.8 ± 0.03. For plotting the adsorption isotherms, different PAC masses (0.25–5 $mg\,L^{-1}$) were added to the buffered Bromacil daughter solution. The solutions were agitated with a magnetic stirrer (5 L reactor) or a recirculation pump (15 L reactor) at a constant temperature of $20 \pm 1\,^{\circ}C$, in the dark, for a contact time of 24 h. Samples were collected and then filtered on fibreglass membranes (Whatman GF/C 1.2 μm filter or Minisart GF/F 0.7 μm syringe) to measure the Bromacil concentrations.

2.1.2. Isotherm for low Bromacil concentrations

Bromacil solutions were prepared under the same conditions as above. However, the volume of purified water needed (250 L) led us to use reverse osmosis water (3–10 $M\Omega\,cm^{-1}$, TOC = 0.1–0.12 $mg\,L^{-1}$) instead of ultrapure water. For adsorption isotherms, different PAC masses (0.1–1 $mg\,L^{-1}$) were added into a 250 L volume reactor containing the Bromacil solutions (initial concentration 4–6 $\mu g\,L^{-1}$, pH 7.8, $I = 1.75 \times 10^{-3}$), for a contact time of 7 days. The solutions were agitated with a blade linked to an electric motor, with a stirring speed of about 400 rpm. Agitation was started an hour before injecting the PAC so as to properly mix the solution. For each sample, 10 times a litre of solution was drawn off and reintroduced into the reactor before sampling the solution for membrane filtration and analysis. Minisart GF/F 0.7 μm fibreglass filters were used.

Table 1
Bibliographic data on the PAC used in this study.

	PAC "SA-UF" from France [12,13]	PAC "SA-UF" from France [5]	PAC "SA-UF" from Netherland [5]
BET surface area	1112 $m^2\,g^{-1}$	1085 $m^2\,g^{-1}$	1112 $m^2\,g^{-1}$
Ashes	8.17%	–	–
Humidity	2%	–	–
Apparent density	0.16 $g\,cm^{-3}$	–	–
Average geometric diameter	6 μm	–	–
Volume of primary micropores (<8 Å)	0.343 $cm^3\,g^{-1}$	0.226 $cm^3\,g^{-1}$	0.214 $cm^3\,g^{-1}$
Volume of secondary micropores (>8 Å)	0.194 $cm^3\,g^{-1}$	–	–
Volume of mesopores (20–500 Å)	0.357 $cm^3\,g^{-1}$	0.885 $cm^3\,g^{-1}$	0.844 $cm^3\,g^{-1}$
Surface area of micropores	733 $m^2\,g^{-1}$	662 $m^2\,g^{-1}$	615 $m^2\,g^{-1}$
Surface area of mesopores	379 $m^2\,g^{-1}$	423 $m^2\,g^{-1}$	421 $m^2\,g^{-1}$

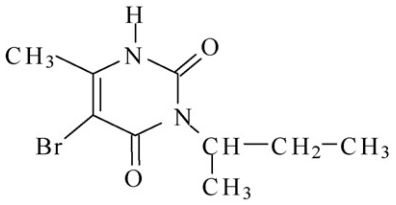

Fig. 1. Bromacil formula.

2.2. Powdered activated carbon

PAC Norit SA-UF powdered activated carbon was used in this study. The pore structure properties (PSPs) were extracted from literature (Table 1) .The PSPs parameters were determined by the N_2 adsorption isotherm technique [4]. It was chosen because of its high mesopore and secondary micropore content and since it is commonly used in drinking water treatment, especially combined with ultrafiltration. The main PAC SA-UF properties may markedly differ depending on the authors and/or manufacturing location (Table 1). It has a net positive charge for pH values below 9.6, which is its zero charge point [14].

2.3. Chemicals

The pesticide studied was Bromacil ($C_9H_{13}BrN_2O_2$, Fig. 1) or 5-bromo-6-methyl-3-[1-methylpropyl]-2,4[1H,3H]-pyrimidinedione of the uracil group.

It was a pure product (98.7%) that is marketed by Fluka-Riedel De Häens (Saint Quentin-Fallavier, France). To check the solution stability, a Bromacil hydrolysis study was carried out at pH 7.8 and 20 °C, for an initial concentration of 3.4 mg L^{-1}. The results showed that the concentration remained stable, even after 22 days, as expected according to the literature [8].

Two sodium salts were used to buffer the ultrapure and reverse osmosis waters:

- sodium phosphate ($NaH_2PO_4{\cdot}H_2O$), 98% purity, marketed by Acros-Organic;
- anhydrous disodium phosphate (Na_2HPO_4) ≥99% purity, marketed by Sigma–Aldrich.

2.4. Analytical procedure

Before each analysis, a standard range was prepared to be able to accurately determine the initial and equilibrium Bromacil concentrations by HPLC coupled with a UV detector. Bromacil analyses were conducted with following equipment set up: Waters 717 injector (200 μL), Hichrom column (reversed phase C_{18}, 5 μm, 250 mm × 4.6 mm); Waters 510 pump (isocratic method), mobile phase with 40% water and 60% methanol with a flow rate of 0.7 mL min^{-1}, Waters 286 UV detector (277 nm), Millennium data acquisition.

A pre-concentration was sometimes necessary, especially for the equilibrium study at low initial concentrations (4–6 μg L^{-1}). In this case, samples (100 mL) were extracted by cartridges (Oasis Waters) and Bromacil was eluted with 2 mL methanol and then diluted with the same amount of ultrapure water (Milli RQ - Milli Q). The yield of extraction (≥97%) and the repeatability (0.5–5%) were determined from solutions of different concentrations (0.1–10 μg L^{-1}) prepared

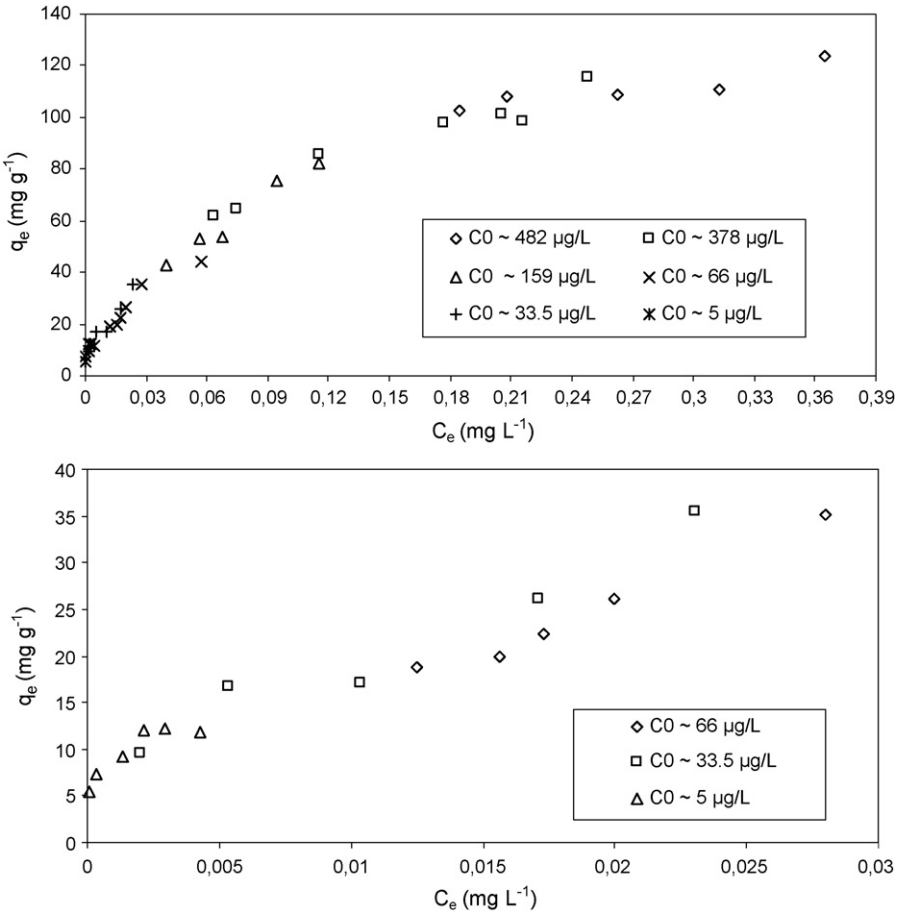

Fig. 2. Bromacil adsorption isotherm in buffered water (pH 7.8) on PAC SA-UF. High: C_0 = 5–482 μg L^{-1} and m_s = 0.1–5 mg L^{-1}. Low: C_0 = 5–66 μg L^{-1} and m_s = 0.1–3 mg L^{-1}.

Table 2
Experimental conditions for Bromacil adsorption isotherms in buffered solution (pH 7.8) on PAC.

Isotherms	Bromacil initial concentration, C_0 ($\mu g\,L^{-1}$)	Volume of solution, V (L)	CAP concentration, m_s (en $mg\,L^{-1}$)
Series 1	482	5	1–1.5–2–2.5–3
Series 2	378	15	1–1.5–2–2.5–3–4–5
Series 3	159	15	0.5–1–1.45–1.9–3
Series 4	66	15	0.5–1–1.5–2–2.5–3
Series 5	33.5	15	0.25–0.5–1.5–2–3
Series 6	5.7	250	0.1–0.2–0.3–0.4–0.6–1

in ultra pure water. The detection limit obtained by this extraction method was 0.05 $\mu g\,L^{-1}$ in pure water.

3. Results and discussion

3.1. General

Six isotherm experiments were carried out with initial Bromacil concentrations (C_0) ranging from 5 to 482 $\mu g\,L^{-1}$ in pure water (DOC = 0.1–0.12 $mg\,L^{-1}$) buffered at pH 7.8 (Table 2). For each experiment, PAC concentrations (Table 2) were selected so that Bromacil adsorption would not exceed ~90% of the initial concentration.

The results were processed in the following form, where q_e vs. (C_e):

$$q_e = \left(\frac{V}{m}\right)(C_0 - C_e) + q_0 \quad (1)$$

Fig. 2 shows all results obtained by isotherm plotting q_e vs. C_e for the six sets of experiments. The plotted curve shows that the isotherm is an L shape, so-called Langmuir [15,16].

3.2. Application of two-parameter models

Our initial objective was to find a two-parameter equation able to modelize the whole of experimental data from C_e = 0.09 $\mu g\,L^{-1}$ to C_e = 364 $\mu g\,L^{-1}$ Five two-parameter models were tested on all data from the experimental isotherm. Their nonlinear and linear forms are presented in Table 3.

The simple and empirical so-called Freundlich model, Eq. (2), is the most commonly used. It applies to many cases, particularly in the case of multilayer adsorption with possible interactions between adsorbed molecules [17].

The Langmuir model, Eq. (3), is also commonly used. Its initial assumptions are that the solid adsorbent has a limited adsorption capacity (q_m), all active sites are identical and they can only complex one solute molecule (monolayer adsorption) [18]. In fact, the Langmuir isotherm is a simple application of the mass action law, leading to the thermodynamic equilibrium constant, which links the concentration of free sites on the adsorbent, the adsorbate concentration in the solution and the concentration of complexed sites at the adsorbent surface.

The Temkin model is based on the assumption that during adsorption gas phase, the adsorption heat, due to interactions with adsorbate, decreases linearly with the recovery rate θ [19]. It is an application of the Gibbs relationship for adsorbents whose surface is considered as energetically homogeneous [20]. Several authors [16,22–26] propose to use this model in the liquid phase in the form indicated in Eq. (5) with q_m of Langmuir.

The Elovich model is based on a kinetic development according to the hypothesis that the adsorption sites increase exponentially with adsorption, involving multi-layered adsorption [27]. It is often used (e.g. [26]) in the form indicated in Eq. (4).

The Dubinin–Radushkevich model (quoted by [28]) does not assume a homogeneous surface or a potential adsorption constant, like the Langmuir model. Its theory of filling the micropore volume is based on the fact that the adsorption potential is variable and that the free adsorption enthalpy is linked to the degree of pore filling. The Dubinin–Radushkevich model is applied to water in the form of Eq. (6).

The linear forms of these two parameter isotherms do not apply to all initial Bromacil concentrations and adsorbent masses used in this study. However, for all linear isotherm expressions studied, it is possible to obtain:

- a right isotherm portion, corresponding to the high equilibrium Bromacil concentrations (~10 $\mu g\,L^{-1} < C_e <$ ~400 $\mu g\,L^{-1}$), with good linear regressions;
- a left isotherm portion, for the low equilibrium Bromacil concentrations of (~0.1 $\mu g\,L^{-1} < C_e <$ ~10 $\mu g\,L^{-1}$), but with a less good linear regression.

The Langmuir (linear form II) and Temkin models gave the best results (Figs. 3 and 4). The parameter values obtained are presented in Table 4, with the Freundlich parameters also mentioned since this

Table 3
The two-parameter equilibrium models tested in this study.

Isotherm	Nonlinear form		Linear form	Plotting
Freundlich	$q_e = K_F C_e^n$	(2)	$\log(q_e) = \log(K_F) + n\log(C_e)$	$\log q_e$ vs. $\log C_e$
Langmuir	$\frac{q_e}{q_m} = \theta = \frac{K_L Ce}{1 + K_L Ce}$	(3)	(Form I) $\frac{1}{q_e} = \frac{1}{C_e}\frac{1}{q_m K_L} + \frac{1}{q_m}$	$\frac{1}{q_e}$ vs. $\frac{1}{C_e}$
			(Form II) $\frac{C_e}{q_e} = C_e\frac{1}{q_m} + \frac{1}{q_m K_L}$	$\frac{C_e}{q_e}$ vs. C_e
			(Form III) $q_e = -\frac{1}{K_L}\frac{q_e}{C_e} + q_m$	q_e vs. $\frac{q_e}{C_e}$
			(Form IV) $\frac{q_e}{C_e} = -K_L q_e + K_L q_m$	$\frac{q_e}{C_e}$ vs. q_e
			(Form V) $\frac{1}{C_e} = K_L q_m \frac{1}{q_e} - K_L$	$\frac{1}{C_e}$ vs. $\frac{1}{q_e}$
Elovich	$\frac{q_e}{q_m} = \theta = K_E C_e \exp - \left(\frac{q_e}{q_m}\right)$	(4)	$\ln\frac{q_e}{C_e} = \ln(K_E q_m) - \frac{q_e}{q_m}$	$\ln\frac{q_e}{C_e}$ vs. q_e
Temkin	$\frac{q_e}{q_m} = \theta = \frac{RT}{\Delta Q}\ln(K_T C_e)$	(5)	$q_e = B_T \ln K_T + B_T \ln C_e$ $\left(\text{with } B_T = \frac{q_m RT}{\Delta Q}\right)$	q_e vs. $\ln C_e$
Dubinin–Radushkevich	$\frac{q_e}{q_m} = \theta = \exp(-\beta\varepsilon^2)$ with $\beta = \frac{1}{E^2}$ and $\varepsilon = RTLn\frac{C_s}{C_e}$	(6)	$\ln q_e = \ln q_{mDR} - \left(\frac{RT}{E}\right)^2 \left(\ln\left(\frac{C_s}{C_e}\right)\right)^2$	$\ln q_e$ vs. $\left(\ln\left(\frac{C_s}{C_e}\right)\right)^2$

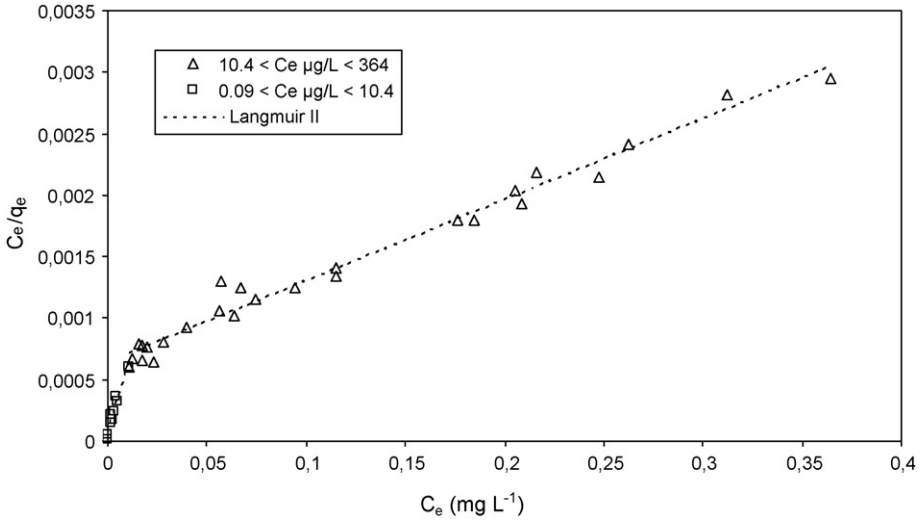

Fig. 3. Application of the Langmuir model (linear form II) for Bromacil adsorption in buffered water (pH 7.8) on PAC SA-UF (C_0 = 5–482 µg L^{-1} and m_s = 0.1–5 mg L^{-1}).

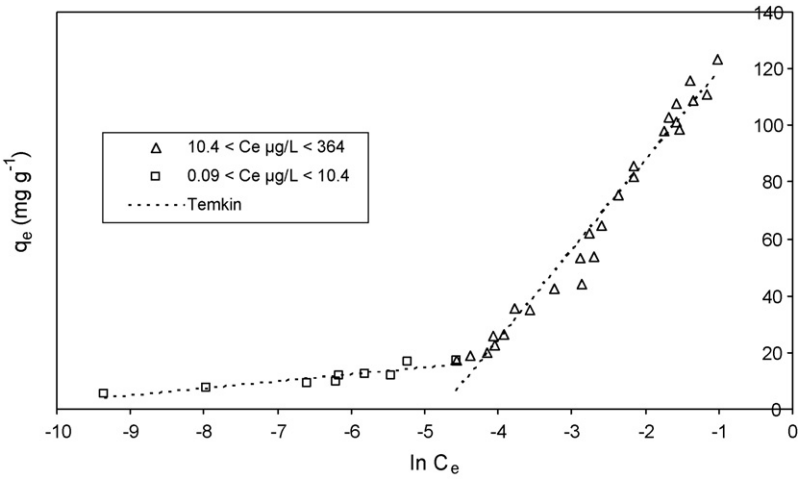

Fig. 4. Application of the Temkin model (linear form) for Bromacil adsorption in buffered water (pH 7.8) on PAC SA-UF (C_0 = 5–482 µg L^{-1} and m_s = 0.1–5 mg L^{-1}).

Table 4
Application of the two-parameter models: equilibrium constants and other parameters.

Freundlich			
10.4 µg L^{-1} ≤ C_e ≤ 364 µg L^{-1}			
Linear form	K_F = 257 mg$^{(1-n)}$ L^n g^{-1}	n = 0.57	r^2 = 0.973
Nonlinear form	K_F = 218 ± 10 mg$^{(1-n)}$ L^n g^{-1}	n = 0.49 ± 0.02	r^2 = 0.966
0.09 µg L^{-1} ≤ C_e ≤ 10.4 µg L^{-1}			
Linear form	K_F = 50 mg$^{(1-n)}$ L^n g^{-1}	n = 0.24	r^2 = 0.858
Nonlinear form	K_F = 59 ± 13 mg$^{(1-n)}$ L^n g^{-1}	n = 0.27 ± 0.04	r^2 = 0.899
Langmuir			
10.4 µg L^{-1} ≤ C_e ≤ 364 µg L^{-1}			
Linear form (II)	q_m = 151.5 mg g^{-1}	K_L = 11 L mg^{-1}	r^2 = 0.981
Nonlinear form	q_m = 154.5 ± 4.8 mg g^{-1}	K_L = 9.7 ± 0.7 L mg^{-1}	r^2 = 0.986
0.09 µg L^{-1} ≤ C_e ≤ 10.4 µg L^{-1}			
Linear form (II)	q_m = 18.1 mg g^{-1}	K_L = 920 L mg^{-1}	r^2 = 0.955
Nonlinear form	n.a.	n.a.	n.a.
Temkin			
10.4 µg L^{-1} ≤ C_e ≤ 364 µg L^{-1}			
Linear form	ΔQ^a = 11.7 kJ mol^{-1}	K_T = 117 L mg^{-1}	r^2 = 0.972
Nonlinear form	ΔQ^a = 11.7 kJ mol^{-1}	K_L = 118.6 ± 9.9 L mg^{-1}	r^2 = 0.972
0.09 µg L^{-1} ≤ C_e ≤ 10.4 µg L^{-1}			
Linear form	ΔQ^a = 18.4 kJ mol^{-1}	K_T = 6.7.10^4 L mg^{-1}	r^2 = 0.831
Nonlinear form	n.a.	n.a.	n.a.

n.a.: not applicable, because standards deviation and confidence intervals too high.
[a] Calculated with q_m from Langmuir II.

Table 5
The three-parameter equilibrium models tested in this study (the three parameters were symbolized by q_m, K_L and n to simplify comparison).

Isotherm	Non linear form		Linear form	Plotting
Redlich–Peterson	$\frac{q_e}{q_m} = \theta = \frac{K_L Ce}{1 + K_L(Ce)^n}$	(7)	$\frac{C_e}{q_e} = \frac{1}{K_L q_m} + \frac{K_L^{(n-1)}}{q_m}(C_e)^n$ $\ln\left(\frac{q_m K_L C_e}{q_e} - 1\right) = n\ln(C_e) + \ln K_L$	$\frac{C_e}{q_e}$ vs. $(C_e)^n$ $\ln\left(\frac{q_m K_L C_e}{q_e} - 1\right)$ vs. $\ln C_e$
Langmuir–Freundlich	$\frac{q_e}{q_m} = \theta = \frac{(K_L Ce)^n}{1 + (K_L Ce)^n}$	(8)	$\frac{q_m}{q_e} = \frac{1}{(K_L Ce)^n} + 1$	$\frac{q_m}{q_e}$ vs. $\frac{1}{C_e^n}$
Sips ou Koble–Corrigan	$\frac{q_e}{q_m} = \theta = \frac{K_L C_e^n}{1 + K_L C_e^n}$	(9)	$\frac{q_m}{q_e} = \frac{1}{K_L C_e^n} + 1$	$\frac{q_m}{q_e}$ vs. $\frac{1}{C_e^n}$
Generalized	$\frac{q_e}{q_m} = \theta = \left(\frac{K_L C_e}{1 + K_L C_e}\right)^n$	(10)	$\left(\frac{q_m}{q_e}\right)^{1/n} = \frac{1}{K_L C_e} + 1$	$\left(\frac{q_m}{q_e}\right)^{1/n}$ vs. $\frac{1}{C_e}$
Tóth	$\frac{q_e}{q_m} = \theta = \frac{K_L Ce}{(1 + (K_L Ce)^n)^{1/n}}$	(11)	$\left(\frac{C_e}{q_e}\right)^n = \left(\frac{1}{q_m}\right)^n \times (C_e)^n + \left(\frac{1}{q_m K_L}\right)^n$	$\left(\frac{C_e}{q_e}\right)^n$ vs. $(C_e)^n$
Fritz–Schluender	$\frac{q_e}{q_m} = \theta = \frac{K_L C_e}{1 + q_m C_e^n}$	(12)	$\frac{C_e}{q_e} = \frac{1}{K_L q_m} + \frac{(C_e)^n}{K_L}$	$\frac{C_e}{q_e}$ vs. $(C_e)^n$
Radke–Prausnitz	$\frac{q_e}{q_m} = \theta = \frac{K_L C_e}{(1 + K_L C_e)^n}$	(13)	$\left(\frac{C_e}{q_e}\right)^{1/n} = \frac{1}{(K_L q_m)^{1/n}} + \frac{(K_L)^{((n-1)/n)} C_e}{(q_m)^{1/n}}$	$\left(\frac{C_e}{q_e}\right)^{1/n}$ vs. (C_e)

model is widely used. An algorithm interpretation using nonlinear regression (SPSS version 14, Levenberg algorithm type – Marquard) was also tested. It generated similar results, especially in the high concentration range.

3.3. Application of three-parameter models

Any two-parameter model can modelize the Bromacil adsorption for the concentration at the equilibrium from $C_e = 0.09\ \mu g\ L^{-1}$ to $C_e = 364\ \mu g\ L^{-1}$. Consequently we tested some three-parameter models (shown in Table 5).

The Redlich–Peterson three-parameter monosolute model is the most quoted and used in the literature since it may be applied over a broad concentration range [16,22,23,26,29–35]. It is an empirical model combining the parameters of the Langmuir and Freundlich equations. This model was initially applied to gas phase adsorption [36]. By analogy, its expression in the liquid phase is the form of Eq. (7) [22,32–34].

The Tóth model is also often cited and used [16,22,23,26,32,34,35,37,38]. This model was developed for the adsorption gas phase [39] on the basis of the Langmuir model, while considering that the adsorbent surface is not energetically homogeneous. This model is of particular interest since it considers that the adsorbent surface is heterogeneous. In the liquid phase, it is generally used as an adaptation of the Langmuir model, close to the empirical Redlich–Peterson model, in the form of Eq. (11).

Many other three-parameter monosolute models are sometimes used, such as Langmuir–Freundlich, Eq. (8), Generalized, Eq. (10), Fritz and Schluender, Eq. (12), and Radke–Prausnitz, Eq. (13) [16,23,26,32,40,41].

The Sips model [42] is not often mentioned [32,43], and it is also sometimes known as the Koble–Corrigan model [31]. It is in the form of Eq. (9) which is generally better validated when $n > 1$. It is possible to determine its expression by applying the mass action law, while considering that n solute molecules are adsorbed per site. In other words, the adsorption reaction stoichiometry would be n solute molecules per free adsorbent site. This interpretation reveals why the n value is generally over 1.

All of these three-parameter models were tested using nonlinear regression algorithms (SPSS version 14, Levenberg algorithm type-Marquard). With the exception of the Redlich–Peterson model, they can all generate a calculated curve that suitably overlaps ($r^2 > 0.97$) the experimental isotherm results. All of these models are therefore able to plot the overall experimental curve. However, each simulation was studied in detail by:

- entering the different model programme values (K_L, n and q_m) in random order;
- applying constraints, including the limits of n ($0 < n < 1$);
- examining the standard errors and 95% confidence intervals;

Table 6
Application of the three-parameter models : equilibrium constants and other parameters.

Model	Form	n	K_L	q_m (mg g^{-1})	r^2
$0.09\ \mu g\ L^{-1} \le C_e \le 364\ \mu g\ L^{-1}$					
Tóth	Nonlinear	0.82 ± 0.09	19.7 ± 8.9	85.2 ± 31.4	0.985
Radke–Prausnitz	Nonlinear	0.80 ± 0.12	19.1 ± 9.0	92.4 ± 33.4	0.984
$10.4\ \mu g\ L^{-1} \le C_e \le 364\ \mu g\ L^{-1}$					
Tóth	Nonlinear	0.94 ± 0.09	11.5 ± 3.2	132.8 ± 32.1	0.986
Tóth	Linear	0.82*	10.2	174	0.982
Radke–Prausnitz	Nonlinear	0.93 ± 0.15	11.7 ± 4.8	133.7 ± 44.1	0.986
Radke–Prausnitz	Linear	0.80*	17.8	93.4	0.983
Fritz–Schluender	Linear	0.80*	10.8	185.2	0.981
$0.09\ \mu g\ L^{-1} \le C_e \le 10.4\ \mu g\ L^{-1}$					
Tóth	Linear	0.82*	1089	18.6	0.958
Radke–Prausnitz	Linear	0.80*	2833	8.8	0.974
Fritz–Schluender	Linear	0.80*	1130	44.2	0.975

* Imposed values for "n"

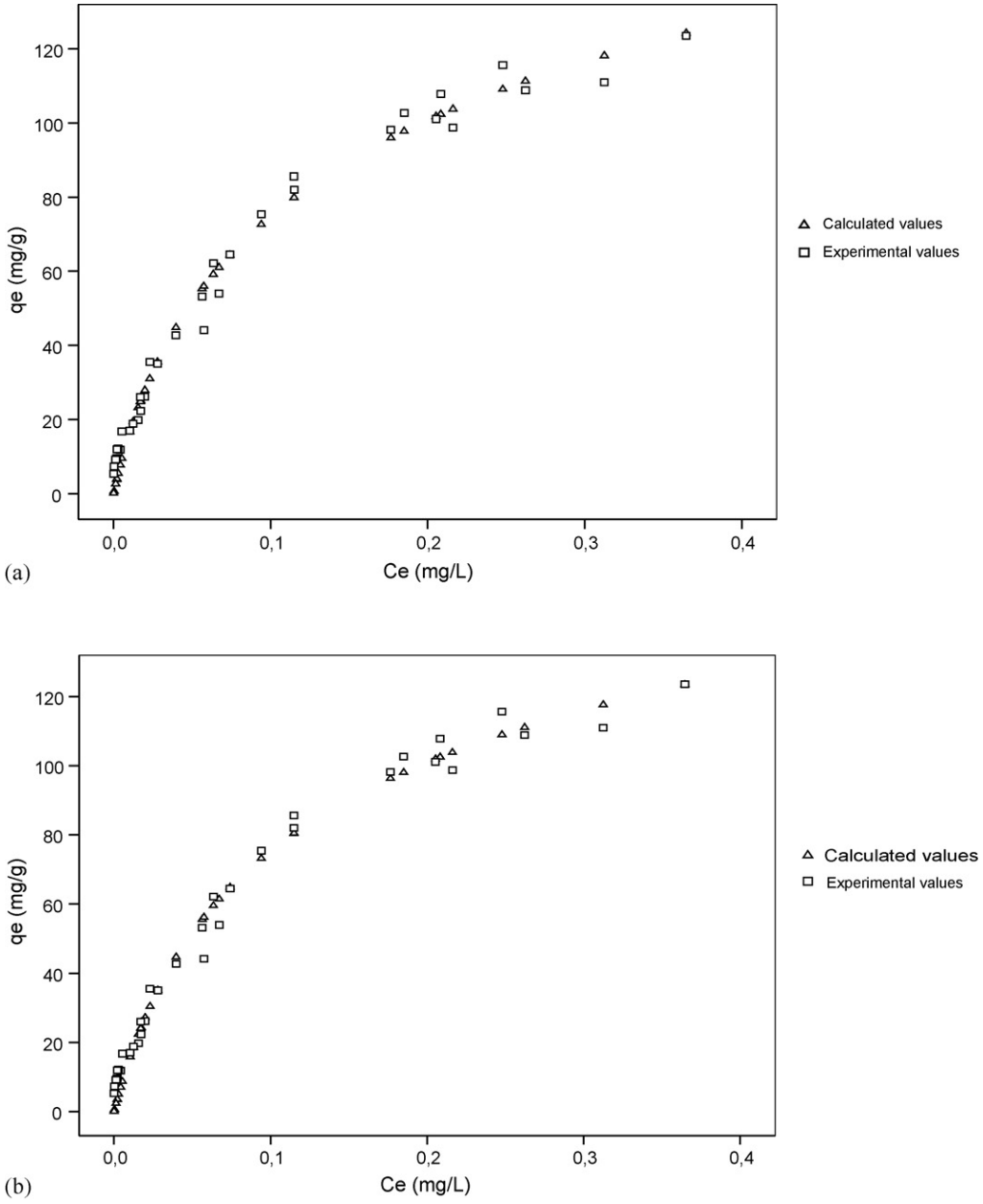

Fig. 5. Application of two three-parameter models [(a) nonlinear Tóth; (b) nonlinear Radke–Prausnitz] for Bromacil adsorption in buffered water (pH 7.8) on PAC SA-UF (C_0 = 5–482 μg L^{-1} and m_s = 0.1–5 mg L^{-1}).

- entering all the experimental values (0.09 μg L^{-1} ≤ C_e ≤ 364 μg L^{-1}), or by range (10.4 μg L^{-1} ≤ C_e ≤ 364 μg L^{-1} or 0.09 μg L^{-1} ≤ C_e ≤ 10.4 μg L^{-1}).

In these conditions, the Tóth and Radke–Prausnitz models were found to perform the best over the entire equilibrium concentration range (Fig. 5).

However, their application in the two separate equilibrium concentration ranges led to different K_L and q_m parameter values (Table 6).

A variant of the nonlinear regression method is to enter the value from one of the three parameters (K_L, q_m, or n) into the model, which then becomes a two-parameter model that can be linearized. The linear forms shown in Table 5 are generally based on the assumption that the n value is known. The best results were obtained with the Tóth (Fig. 6), Radke–Prausnitz and Fritz–Schluender models, as shown in Table 6.

3.4. Discussion on the equilibrium isotherm

With regard to possible practical applications of water treatment, it is the use of nonlinear models "Tóth" and "Radke–Prausnitz" models that would best modelize the adsorption equilibrium on the concentration range studied.

Regarding the application of other models in their linear forms (Freundlich, Langmuir II, Temkin and Tóth), one possible interpretation of all of the obtained data is that the studied activated carbon has two groups (or types) of active sites for Bromacil:

- very reactive sites, called A sites, which are weakly present at the surface of PAC and which react in a first stage (these A sites are the only ones that complex Bromacil at very low concentration);
- less active sites, called B sites, strongly present at the PAC surface, which react in a second stage when the A sites are saturated (in the presence of high Bromacil concentrations, most reactions concern

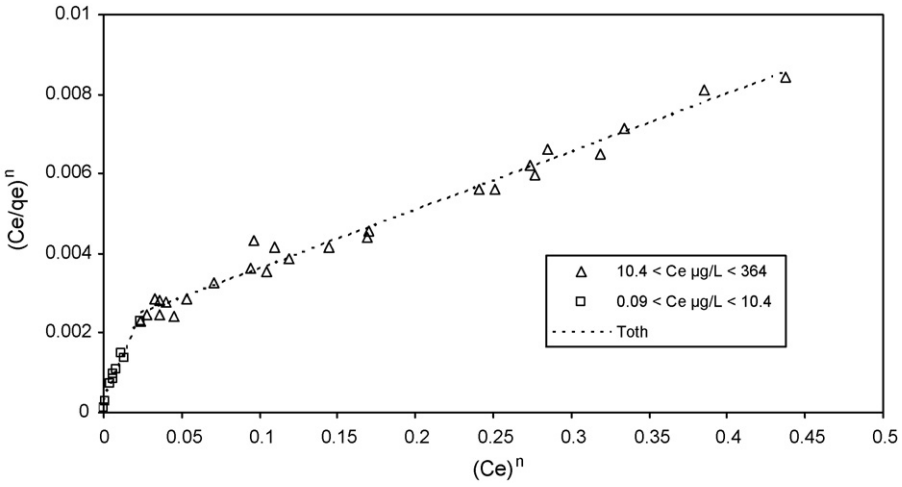

Fig. 6. Application of the Tóth three-parameter model, under its linear form (with $n = 0.82$) for Bromacil adsorption in buffered water (pH 7.8) on PAC SA-UF (C_0 = 5–482 µg L^{-1} and m_s = 0.1–5 mg L^{-1}).

these B sites while masking the reaction of A sites, and then their equilibrium parameters).

The sorption phenomenon is linked to site reactivity but also to the intra-particle distribution. Another interpretation is based on the fact that adsorption is limited to the most accessible pores at very low solute concentrations. For high equilibrium concentrations, only access to other pores (less readily available, but much more present) can make it possible to achieve high adsorption capacities that mask the first type of adsorption.

All model parameters (Tables 3 and 5) were in line with these two assumptions. The n (Freundlich) values between 0.1 and 0.5 (for A sites) reflected good adsorption, while adsorption was considered moderate for n values between 0.5 and 1 (for B sites) [21,44].

The equilibrium constant values (K_L of the Langmuir, Tóth, Radke–Prausnitz and Fritz–Schluender models) were significantly higher for A sites ($\sim 10^3$ L mg^{-1}) than for B sites (10–20 L mg^{-1}), as well as for the K_T constant and the heat of adsorption (ΔQ) of the Temkin model. These data demonstrate that the A sites had greater reactivity. However, the q_m values showed a much higher presence (or concentration) of B sites on the adsorbent surface.

The application of the two-site Langmuir model, Eq. (14), (mass action law with two types of sites) again confirmed these hypotheses of two different reactivity and concentration sites (or pores) on the PAC.

$$\frac{q_e}{q_m} = \theta = \left[\frac{f_A K_{LA} C_e}{1 + K_{LA} C_e} + \frac{f_B K_{LB} C_e}{1 + K_{LB} C_e}\right] \quad (14)$$

With average values of $K_{LA} \sim 1000$ L mg^{-1}, $K_{LB} \sim 10$ L mg^{-1} and q_m = 151 mg g^{-1} (extracted from previous data), this application led to Fig. 7 and the following parameters:

$$f_A = 0.031 \pm 0.011$$

$$f_B = 0.956 \pm 0.023$$

$$r^2 = 0.986$$

The surface of a Bromacil molecule is approximately 100 Å^2 [45], which corresponds to 2.3 mg of Bromacil per m^2. According to the literature (Table 1), the average total specific surface is about 1100 m^2 g^{-1}, but 60–65% of this surface corresponds to micropores (diameter <8 Å) that are theoretically not accessible to

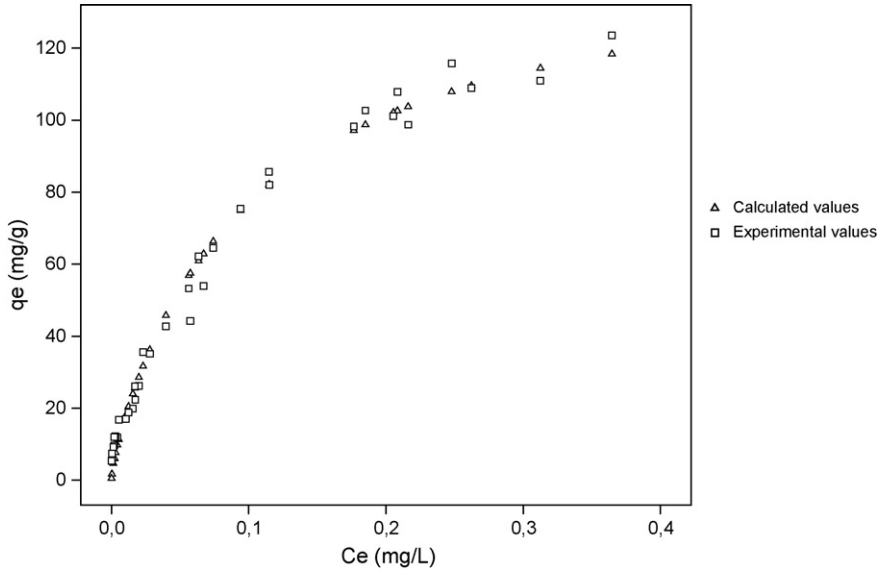

Fig. 7. Application of the "Langmuir – 2 sites" model for Bromacil adsorption in buffered water (pH 7.8) on PAC SA-UF (C_0 = 5–482 µg L^{-1} and m_s = 0.1–5 mg L^{-1}).

Bromacil. The maximum capacity for monolayer adsorption of the studied PAC compared to the surface of Bromacil molecule would be between 170 mg g^{-1} and 190 mg g^{-1}. This theoretical value is very close to the experimental q_m values obtained, including those using linearized forms of the Langmuir, Tóth and Fritz–Schluender models.

4. Conclusion

The main feature of our study is that it was carried out with a very broad range of initial solute concentrations (~5 μg L^{-1} to ~500 μg L^{-1}), and thus relatively high PAC concentrations (0.1–5 mg L^{-1}). The application of several mono-solute equilibrium models (with two, three or more parameters) generally showed that Bromacil adsorption probably occurred on two types of site. At very low adsorbate concentration (<10 μg L^{-1} in our case), they were high reactivity free sites or pores ($K_L \sim 10^3$ L mg^{-1}) that reacted. When the initial adsorbate concentration was higher, a large proportion of this concentration was mostly adsorbed on lower reactivity free sites ($K_L \sim 10$ L mg^{-1}). In this case, the experimental approach measured only this type of adsorption, with markedly different K_L and q_m values as compared to those of the first stage. In this latter case, the magnitude of q_m corresponded to almost total coverage of the area occupied by activated carbon secondary micropores and mesopores. The ratio between the site concentrations was about 10–20 according to the q_m values calculated by the two- or three-parameter models, or more (between 30 and 40) according to the two-site Langmuir model. In the second part of this paper, kinetic studies were carried out to assess these two types of site.

Acknowledgments

This study was conducted at the Laboratory of Chemistry and Microbiology of Water (CNRS UMR 6008) of the Engineering Institute of Poitiers in the University of Poitiers in France with the financial support from the University of Damascus in Syria.

References

[1] Commission of the European Communities, Council directive concerning the quality of water intended for human consumption, 98/83/CE, November 3, 1998.
[2] D.R.U. Knappe, Y. Matsui, V.L. Snoeyink, P. Roche, M.J. Prados, M.M. Bourbigot, Predicting the capacity of powdered activated carbon for trace organic compounds in natural waters, Environmental Science and Technology 32 (1998) 1694–1698.
[3] L.C. Schideman, V.L. Snoeyink, B.J. Mariñas, L. Ding, C. Campos, Application of a three-component competitive adsorption model to evaluate and optimize granular activated carbon systems, Water Research 41 (2007) 3289–3298.
[4] Q. Li, V.L. Snoeyink, C. Campos, B.J. Mariñas, Displacement effect of NOM on atrazine adsorption by PACs with different pore size distributions, Environmental Science and Technology 36 (2002) 1510–1515.
[5] L. Ding, B.J. Mariñas, L.C. Schideman, V.L. Snoeyink, Competitive effects of natural organic matter: parametrization and verification of the three-component adsorption model Compsorb, Environmental Science and Technology 40 (2006) 350–356.
[6] M. Campinas, M.J. Rosa, The ionic strength effect on microcystin and natural organic matter surrogate adsorption onto PAC, Journal of Colloid and Interface Science 299 (2006) 520–529.
[7] G.D. Clayton, F.E. Clayton, Patty's Industrial Hygiene and Toxicology. 2. Toxicology, third edition, John Wiley and Sons, NY, 1981.
[8] Y.T. Das, Hydrolysis of Bromacil in Aqueous Solutions Buffered at pH 5, 7, and 9: Project No.86001-02; DuPont Document No. AMR-522-86, unpublished study prepared by Biospherics Inc., 1988, 33 pp.
[9] R.G. Vandriesche, Pesticide profiles: Bromacil, Cooperative Extension Service, Department of Entomology, University of Massachusetts, Cooperative Extension Service, Amherst, MA, 1985.
[10] U.S. EPA, Bromacil: Health Advisory. Office of Drinking Water, Washington, DC, 1988.
[11] DIREN, Suivi des pesticides, Etat de la contamination dans les milieux aquatiques en Martinique, Communication Orale, séance plénière de la CERPE, Décembre, 2003.
[12] C. Campos, L. Schimmoller, B.J. Mariñas, V.L. Snoeyink, I. Baudin, J.-M. Laîné, Adding PAC to remove DOC, Journal of American Water Works Association 92 (2000) 69–83.
[13] Q. Li, V.L. Snoeyink, B.J. Mariñas, C. Campos, Pore blockage effect of NOM on atrazine adsorption kinetics of PAC: the roles of NOM molecular weight and PAC pore size distribution, Water Research 37 (2003) 4863–4872.
[14] M. Bjelopavlic, G. Newcombe, J. Hayes, Adsorption of NOM onto activated carbon: effect of surface charge, ionic strength, and pore volume distribution, Journal of Colloid and Interface Science 210 (1999) 271–280.
[15] C.H. Giles, D. Smith, A. Huitson, A general treatment and classification of the solute adsorption isotherm. I. Theoretical, Journal of Colloid and Interface Science 47 (1974) 755–765.
[16] C. Hinz, Description of sorption data with isotherm equations, Geoderma 99 (2001) 225–243.
[17] H. Freundlich, Kapillarchemie. Akademische Verlagsgesellschaft, Leipzig, Germany, 1909.
[18] I. Langmuir, The adsorption of gases on plane surfaces of glass, mica and platinum, Journal of American Chemical Society 40 (1918) 1361–1403.
[19] M.J. Tempkin, V. Pyzhev, Kinetics of ammonia synthesis on promoted iron catalysts, Acta Physicochimica 12 (1940) 217–256.
[20] J. Toth, State equations of the solid gas interface layer, Acta Chemistry Academia Science 69 (1971) 311–328.
[21] O. Hamdaoui, Batch study of liquid-phase adsorption of methylene blue using cedar sawdust and crushed brick, Journal of Hazardous Materials B 135 (2006) 264–273.
[22] V.C. Srivastava, M.M. Swamy, D. Malli, B. Prasad, I.M. Mishra, Adsorptive removal of phenol by bagasse fly ash and activated carbon: equilibrium, kinetics and thermodynamics, Journal of Colloids and Surfaces A: Physicochemical and Engineering Aspects 272 (2006) 89–104.
[23] G. Limousin, J.P. Gaudet, L. Charlet, S. Szenknect, V. Barthes, M. Krimissa, Sorption isotherms: a review on physical bases, modeling and measurement, Journal of Applied Geochemistry 22 (2007) 249–275.
[24] B.H. Hameed, Equilibrium and kinetic studies of methyl violet sorption by agricultural waste, Journal of Hazardous Materials 154 (2007) 204–212.
[25] O. Hamdaoui, E. Naffrechoux, Modeling of adsorption isotherms of phenol and chlorophenols onto granular activated carbon. Part I. Two-parameter models and equations allowing determination of thermodynamic parameters, Journal of Hazardous Materials 147 (2007) 381–394.
[26] F. Gimbert, N.M. Crini, F. Renault, P.M. Badot, G. Crini, Adsorption isotherm models for dye removal by cationized starch-based material in a single component system: error analysis, Journal of Hazardous Materials 157 (2008) 34–46.
[27] S.Y. Elovich, O.G. Larinov, Theory of adsorption from solutions of non-electrolytes on solid (I) equation adsorption from solutions and the analysis of its simplest form (II), verification of the equation of adsorption isotherm from solutions, Izvestiya of the Academy of Science of the USSR, Physical Chemistry 2 (1962) 209–216.
[28] L.J. Kennedy, J.J. Vijaya, K. Kayalvizhi, G. Sekaran, Adsorption of phenol from aqueous solutions using mesoporous carbon prepared by two-stage process, Journal of Chemical Engineering 132 (2007) 279–287.
[29] K.H.H. Choy, J.F. Porter, G. Mc kay, Single and multicomponent equilibrium studies for the adsorption of acidic dyes on carbon from effluents, Langmuir 20 (2004) 9646–9656.
[30] B. Özkaya, Adsorption and desorption of phenol on activated carbon and a comparison of isotherm models, Journal of Hazardous Materials 129 (2006) 158–163.
[31] D. Karagag, Modeling the mechanism, equilibrium and kinetics for the adsorption of Acid Orange 8 onto surfactant-modified clinoptilolite: the application of nonlinear regression analysis, Journal of Dyes and Pigments 74 (2007) 659–664.
[32] O. Hamdaoui, E. Naffrechoux, Modeling of adsorption isotherms of phenol and chlorophenols onto granular activated carbon. Part II. Models with more than two parameters, Journal of Hazardous Materials 147 (2007) 401–411.
[33] M.C. Ncibi, Applicability of some statistical tools to predict optimum adsorption isotherm after linear and non-linear regression analysis, Journal of Hazardous Materials 153 (2008) 207–212.
[34] A. Kumar, S. Kumar, S. Kumar, D.V. Gupta, Adsorption of phenol and 4-nitrophenol on granular activated carbon in basal salt medium: equilibrium and kinetics, Journal of Hazardous Materials 147 (2007) 155–166.
[35] R.K. Singh, S. Kumar, S. Kumar, A. Kumar, Development of parthenium based activated carbon and its utilization for adsorptive removal of p-cresol from aqueous solution, Journal of Hazardous Materials 155 (2008) 523–535.
[36] O. Redlich, D.L.A. Peterson, Useful adsorption isotherm, Journal of Physical Chemistry 63 (1959) 1024–1026.
[37] I. Pikaar, A.A. Koelmans, P.C.M. Van Noort, Sorption of organic compounds to activated carbons. Evaluation of isotherm models, Chemosphere 65 (2006) 2343–2351.
[38] W. Rudzinski, W. Plazinski, Theoretical description of the kinetics of solute adsorption at heterogeneous solid/solution interfaces on the possibility of distinguishing between the diffusional and the surface reac-

tion kinetics models, Journal of Applied Surface Science 253 (2007) 5827–5840.
[39] J. Toth, Gas- (Dampt) – adsorption an festen oberflächen in homogener aktivität III, Acta Chimica Hungarica 32 (1962) 39–45.
[40] W. Fritz, E.U. Schluender, Simultaneous adsorption equilibrium of organic solutes in dilute aqueous solution on activated carbon, Journal of Chemical Engineering Science 29 (1974) 1279–1282.
[41] C.J. Radke, J.M. Prausnitz, Adsorption of organic solutions from dilute aqueous solution on activated carbon, Industrial and Engineering Chemistry Fundamentals 11 (1972) 445–451.
[42] R. Sips, On the structure of a catalyst surface, The Journal of Chemical Physics 16 (1948) 490–495.
[43] Y. Jin, K.H. Row, Adsorption isotherm of Ibuprofen on molecular imprinted polymer, Journal of Chemical Engineering 22 (2005) 264–267.
[44] R.E. Treybal, Mass-Transfer Operations, third ed., McGraw-Hill, 1981.
[45] R.S. Baughman, P.J. Yu, Crystal and molecular structure of herbicides: bromacil (Hyvar), Journal of Agriculture and Food Chemistry 36 (1988) 1294–1296.